

Matthew Birney<sup>1</sup>, Emma Whelan<sup>1</sup>, Catherine Dougados<sup>2</sup>,  
Sylvie Cabrit<sup>3</sup>, Brunella Nisini<sup>4</sup>, Jochen Eisloffel<sup>5</sup>

<sup>1</sup>Department of Experimental Physics, Maynooth University, Ireland; <sup>2</sup>IPAG, Université Grenoble Alpes, France; <sup>3</sup>Observatoire de Paris, Paris Sciences et Lettres University, France; <sup>4</sup>Osservatorio Astronomico di Roma, INAF, Italy; <sup>5</sup>Thüringer Landessternwarte Tautenburg, Germany

## Abstract

**Outflows** from young stellar objects (YSO's) play a key role in star formation. Jets play a role in the mass and angular momentum extraction of the forming star but are also thought to **impact on the planet forming regions of this disk**. However, the precise theoretical model for jet launching is currently debated. This poster presents results on the kinematics and morphology of the **HH 46/47** jet using ESO's Integral-Field Spectroscopy (IFS) instruments; **MUSE** and **SINFONI**. These instruments allow the simultaneous observations of many optical and NIR Forbidden Emission Lines (FEL's) and Molecular Hydrogen Emission Lines (MHEL's) over large spatial ranges. I seek to provide constraints to theoretical models explaining the mechanics of jets. By understanding how jets are launched and how they interact with the circumstellar disks within which planets form, their role in the planet formation process will be better understood.

## Introduction

- Stars form inside large molecular gas clouds. They eject material in energetic bipolar MHD (magnetohydrodynamic) winds that have two components; **1. Collimated components (Jets); 2. Wide-angle components.**
- Outflows remove angular momentum from the circumstellar disk as material accretes onto the driving source.
- HH 46/47:**
  - Collection of Herbig-Haro (HH) objects located in a dense Bok Globule in the Gum nebula ( $d = 450$  pc) in the southern sky.
  - Bright blueshifted jet extends out of globule relatively unobscured.
  - Faint redshifted counter-jet extends into globule.
  - Outflow driven by **HH 46 IRS**: Young, class I YSO,  $L = 12 L_{\odot}$ , binary system (separation =  $0.26''$ )
  - $\theta_j = 31^{\circ}$  (plane of sky).
  - Average jet velocity =  $300 \text{ km s}^{-1}$ .

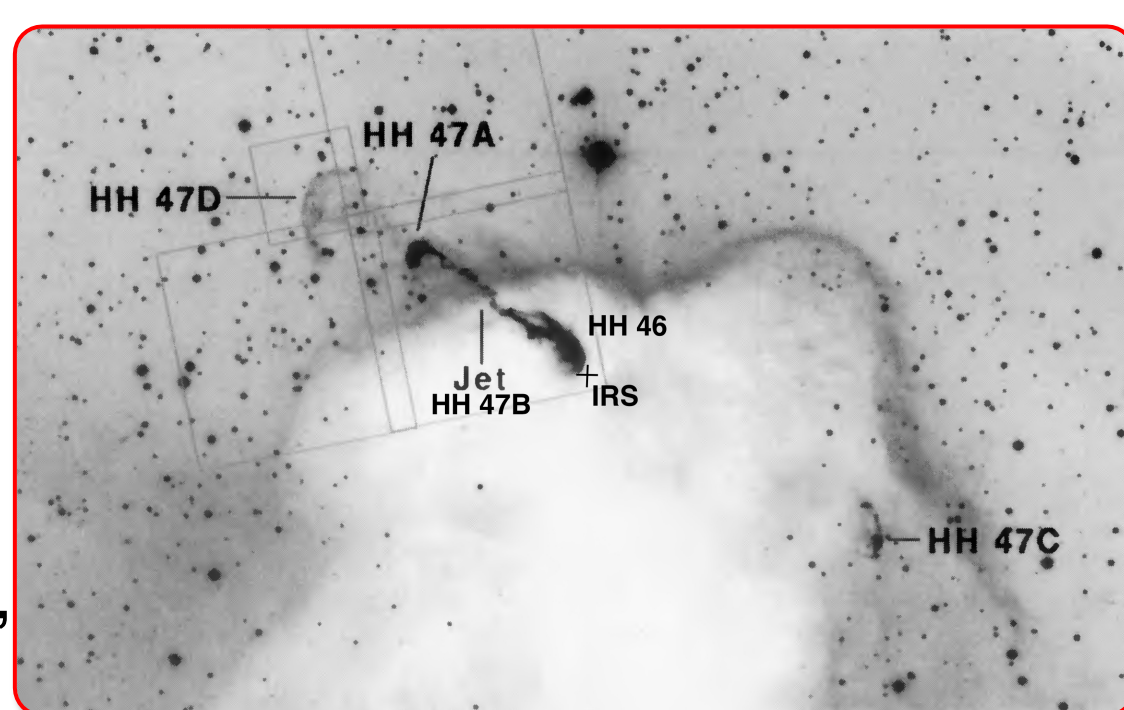


Fig 1: HH 46/47 system (Stanke, 1999)

## Observations & Data Reduction

Observations were obtained using ESO's IFS instruments MUSE (Multi-Unit Spectroscopic Explorer) and SINFONI (Spectrograph for INtegral Field Observations in the Near Infrared) which are both installed on the VLT at Paranal Observatory, Chile. ESO programme ID: 0102-0615(A) (PI C.Dougados). IFS instruments produce *datacubes*, where the signal from each pixel is sent to a spectrograph generating a spectrum for every individual pixel.

- MUSE:** Data was obtained using the instruments Wide Field Mode ( $1.0' \times 1.0'$ ) with a spatial resolution of  $0.2''/\text{pixel}$  with no AO. The observation ranges in wavelength from  $470 \text{ nm} - 935 \text{ nm}$ . Spectral resolution varies from 1700 in the blue end of the wavelength range to 3400 in the red end. This wide FOV is suited to map the entire extent of the jet's inner cavity. AO was not used to enhance the angular resolution and the S/N ratio.
- SINFONI:** Data was obtained using the instruments K-band grating ( $1.95 \mu\text{m} - 2.45 \mu\text{m}$ ) with an FOV of  $8'' \times 8''$  and a spatial resolution of  $0.25''/\text{pixel}$ . Spectral resolution in the K-band is 4000 and no AO was used. This FOV is well matched to typical sizes of wide-angle outflow cavities.

MUSE data comes pre-reduced and calibrated from ESO. The SINFONI data was reduced using ESO's data reduction pipeline *EsoReflex*. The datacube was corrected for bad pixels, dark field, flat field, geometric distortions on the detector and night sky emission. Continuum subtraction was performed around emission lines of interest. SINFONI wavelength calibration was done using *EsoReflex* and further calibrated using OH sky-lines for greater accuracy.

The SINFONI data was flux calibrated using standard stars HD 67954 and HD 73105. The stars' known magnitudes in the J, H and K bands were converted to flux densities using equation 1. Here  $F_0(\text{Band})$  is the zero-magnitude flux of a star in a particular band and  $m(\text{Band})$  is the known magnitude of the star. A flux calibration curve was derived from the standard stars' fluxes and applied to every spectrum in the cube converting pixel values from arbitrary detector counts to physical flux units.

$$F_{\text{calib}}(\text{Star}) = F_0(\text{Band}) \times 10^{-m(\text{Band})/2.5} \quad (1)$$

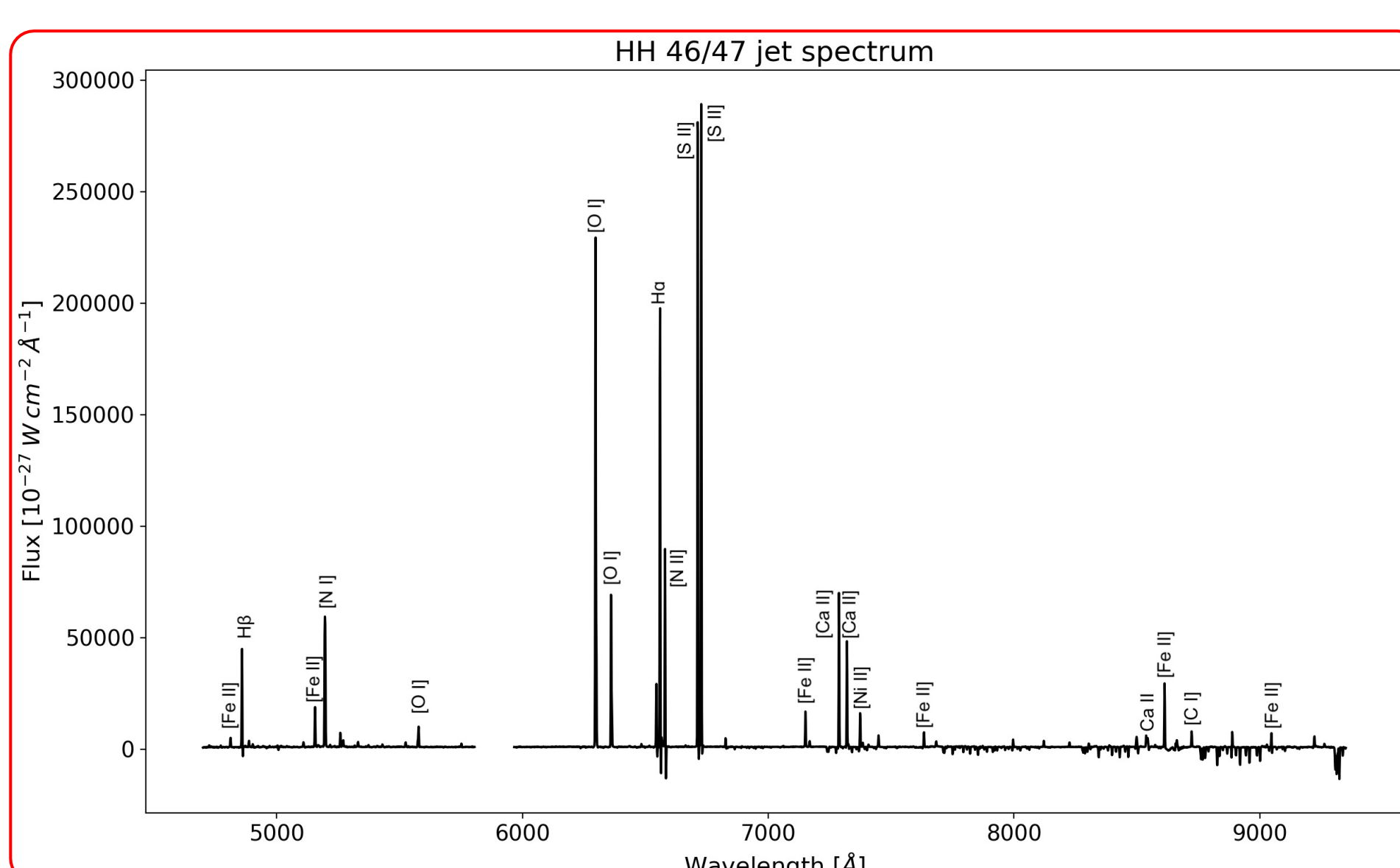


Fig 2: Jet emission spectrum extracted from MUSE data (optical). Bright emission lines are labelled.

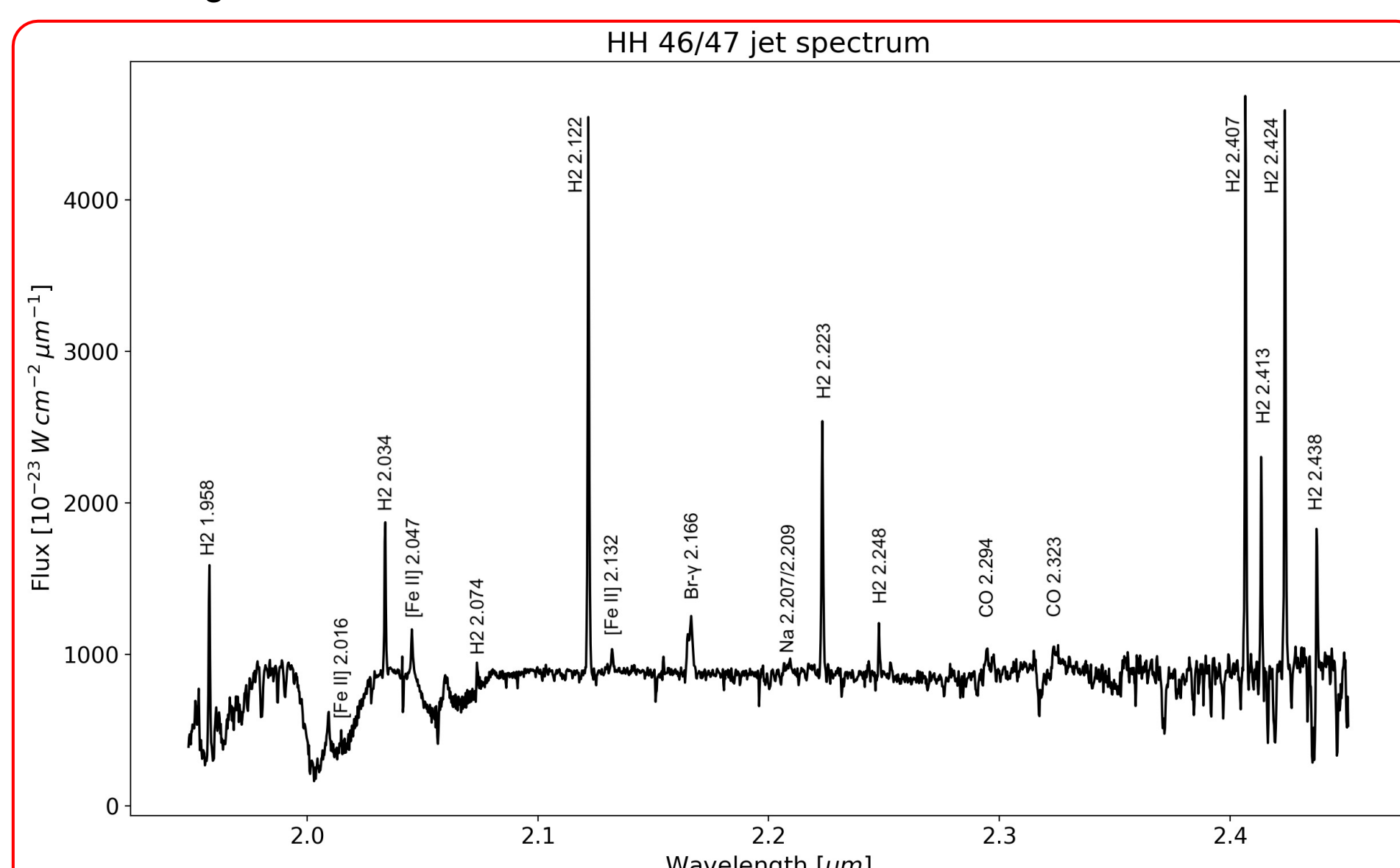


Fig 3: Jet emission spectrum extracted from SINFONI data (NIR). Bright emission lines are labelled.

$\lambda_{\text{Air}} (\text{\AA})$	Ion	$\lambda_{\text{Air}} (\text{\AA})$	Ion
4814.54415	[Fe II]	7171.9985	[Fe II]
4861.325	H I	7291.47	[Ca II]
4889.62268	[Fe II]	7323.89	[Ca II]
4905.35139	[Fe II]	7377.83	[Ni II]
5111.63640	[Fe II]	7388.1673	[Fe II]
5158.7924	[Fe II]	7452.5611	[Fe II]
5197.9016	[N I]	7637.5153	[Fe II]
5220.0757	[Fe II]	7686.9261	[Fe II]
5261.6327	[Fe II]	8000.08	[Cr II]
5273.3634	[Fe II]	8125.30	[Cr II]
5333.6610	[Fe II]	8229.67	[Cr II]
5376.4657	[Fe II]	8308.49	[Cr II]
5527.3536	[Fe II]	8542.09	Ca II
5577.338	[O I]	8578.70	[Cl II]
5754.64	[N II]	8616.9498	[Fe II]
6300.304	[O I]	8662.14	Ca II
6363.776	[O I]	8727.13	[C I]
6548.04	[N II]	8891.9283	[Fe II]
6562.80	H I	9033.4909	[Fe II]
6583.46	[N II]	9051.9510	[Fe II]
6716.44	[S II]	9226.6267	[Fe II]
6730.82	[S II]	9267.5547	[Fe II]
7155.1742	[Fe II]		

Table 1: Identified emission lines in MUSE data and their rest wavelengths.

## Acknowledgements

I am extremely grateful to my supervisor Dr Emma Whelan and the Experimental Physics department at Maynooth University. Thank you to C. Dougados, S. Cabrit, B. Nisini and J. Eisloffel for their expertise and assistance. This work is sponsored by the Hume Doctoral awards and National University of Ireland (NUI).

## Results

### Spectro-images/channel maps (SINFONI data):

- Channel maps of the blueshifted jet cavity. Maps are rotated clockwise by  $142.3^{\circ}$  so that the jet axis lies along the horizontal (Jet PA =  $52.3^{\circ}$ ). The red circle marks the position of the ALMA mm continuum peak.

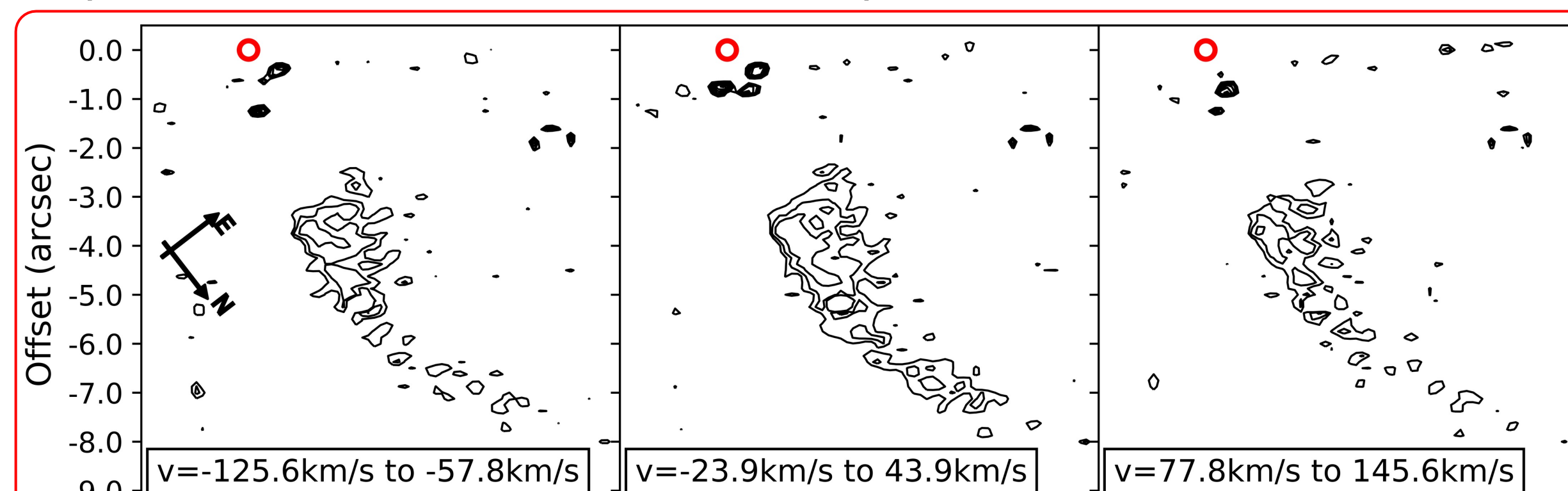


Fig 4: H2 2.12  $\mu\text{m}$  channel maps. Contours start at  $2\sigma$  and increase by factors of 1.5.  $\sigma$  ranges from  $36.37 - 102.60 (\times 10^{-23} \text{ W cm}^{-2} \mu\text{m}^{-1} \text{ pixel}^{-1})$

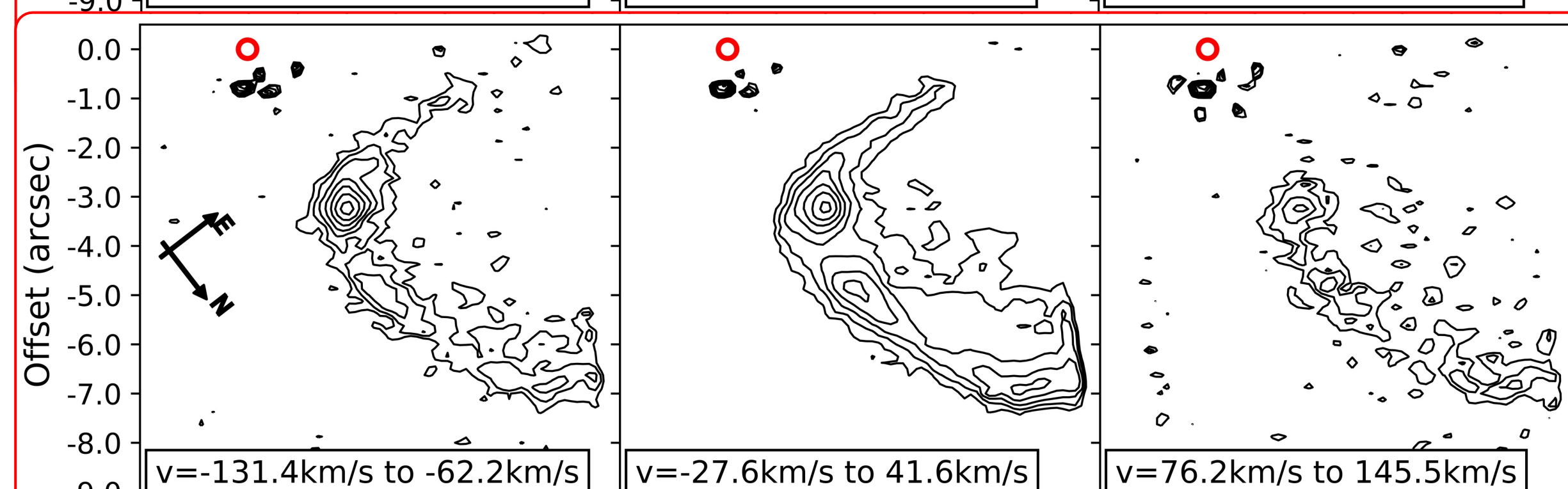


Fig 5: Br- $\gamma$  (2.17  $\mu\text{m}$ ) channel maps. Contours start at  $2\sigma$  and increase by factors of 1.5.  $\sigma$  ranges from  $40.93 - 50.30 (\times 10^{-23} \text{ W cm}^{-2} \mu\text{m}^{-1} \text{ pixel}^{-1})$

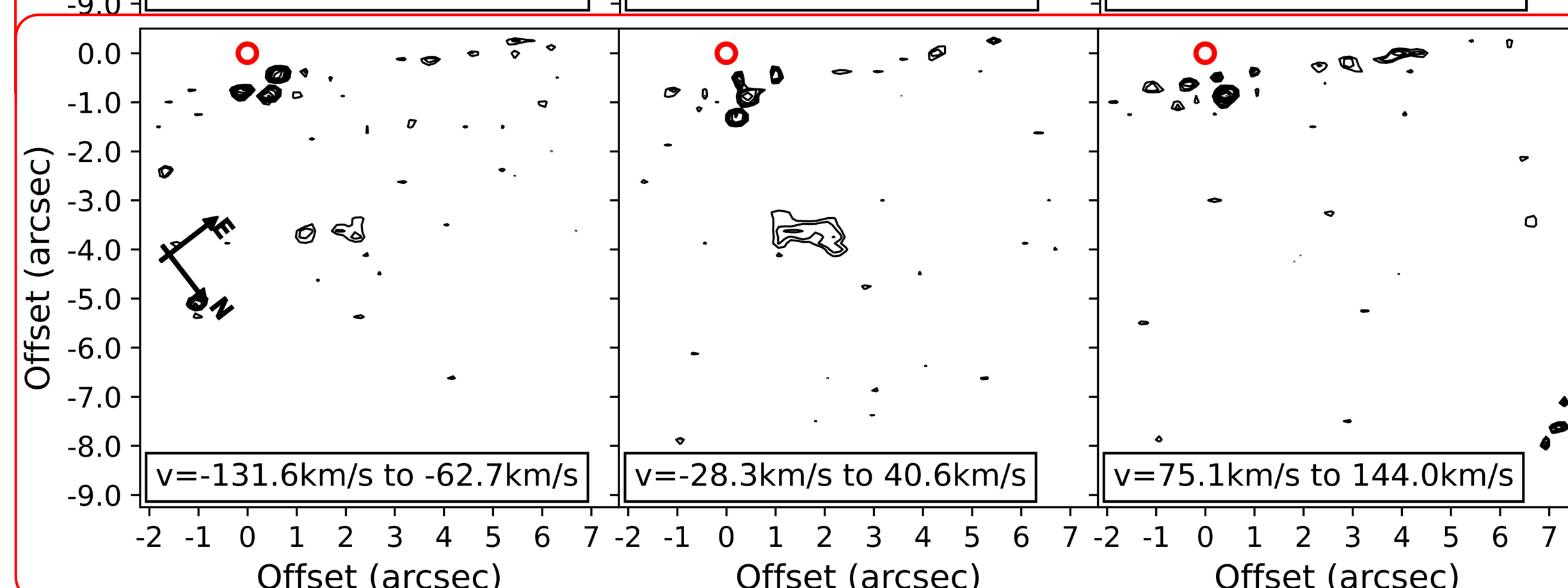


Fig 6: [Fe II] 2.13  $\mu\text{m}$  channel maps. Contours start at  $2\sigma$  and increase by factors of 1.5.  $\sigma$  ranges from  $24.16 - 28.08 (\times 10^{-23} \text{ W cm}^{-2} \mu\text{m}^{-1} \text{ pixel}^{-1})$

### Position-velocity diagrams: (Velocities are LSR velocities)

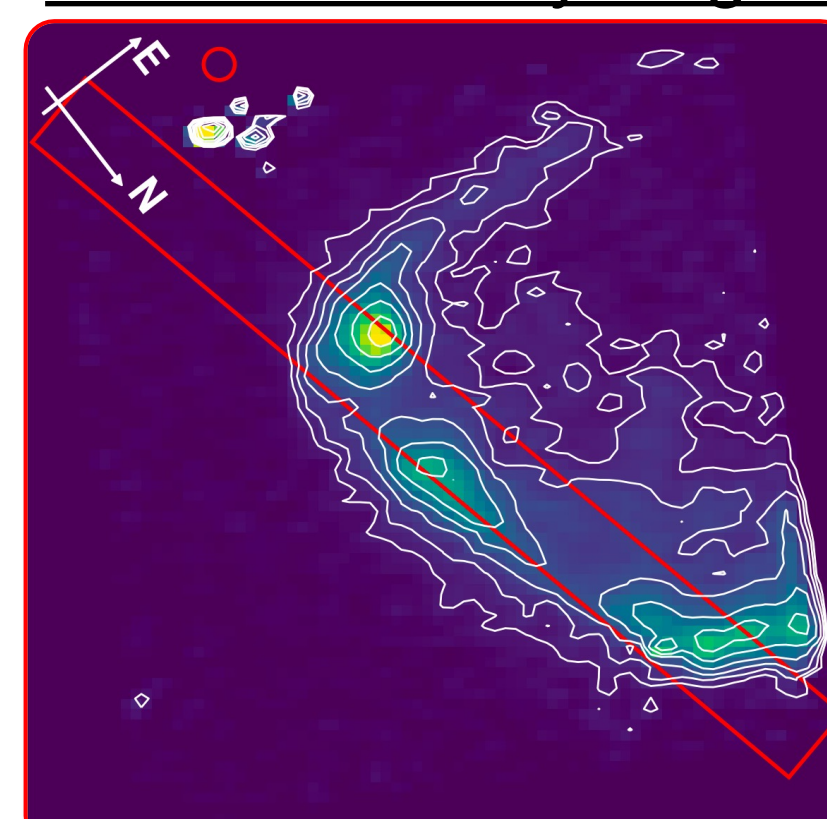


Fig 7: Slit position (width =  $1''$ ) for extracting PV diagrams. (H2 2.12 emission shown for reference)

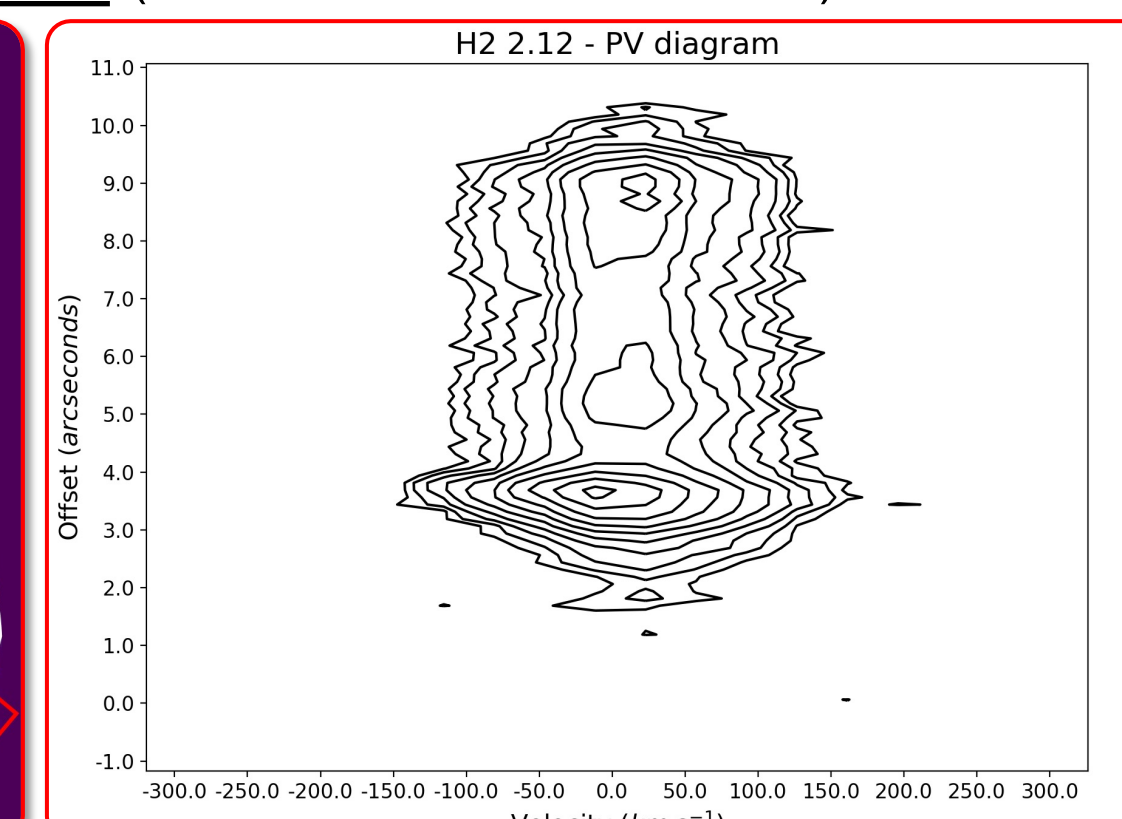


Fig 8: H2 2.12 PV diagram. Contours start at  $3\sigma$  and increase by factors of 1.5 ( $\sigma = 44.25 \times 10^{-23} \text{ W cm}^{-2} \mu\text{m}^{-1} \text{ pixel}^{-1}$ )

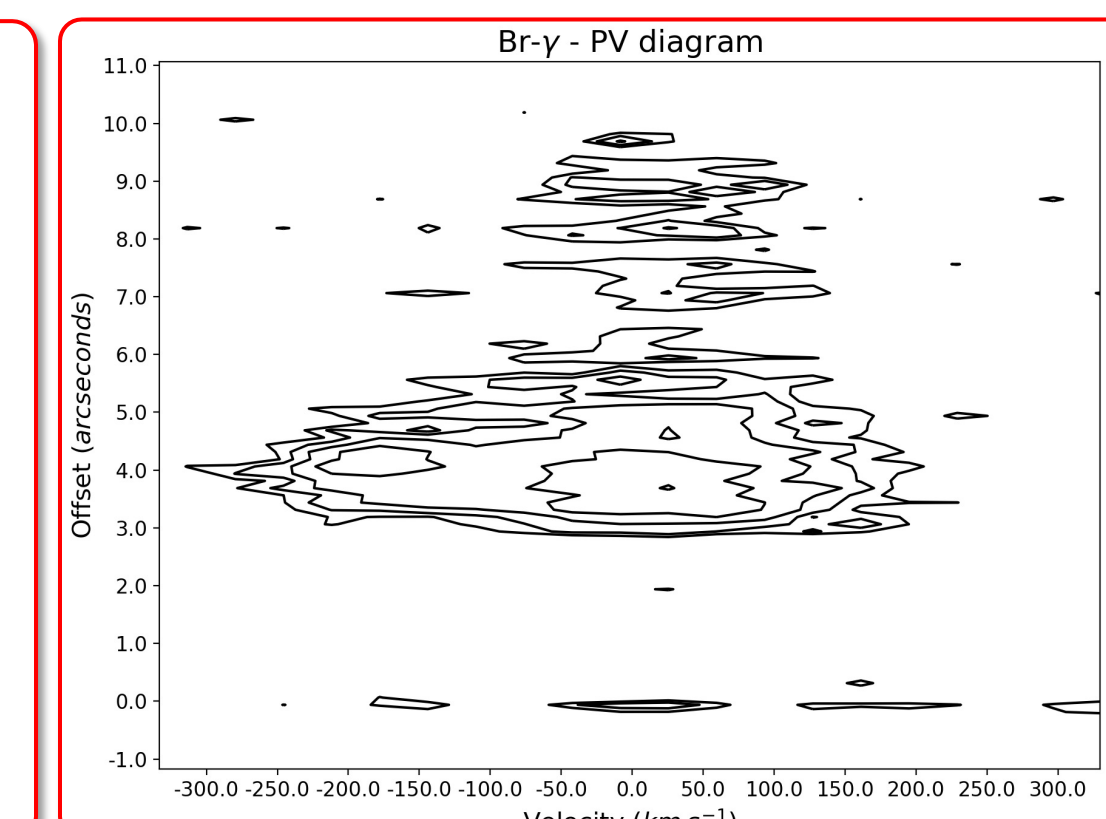


Fig 9: Br- $\gamma$  PV diagram. Contours start at  $3\sigma$  and increase by factors of 1.5 ( $\sigma = 43.56 \times 10^{-23} \text{ W cm}^{-2} \mu\text{m}^{-1} \text{ pixel}^{-1}$ )

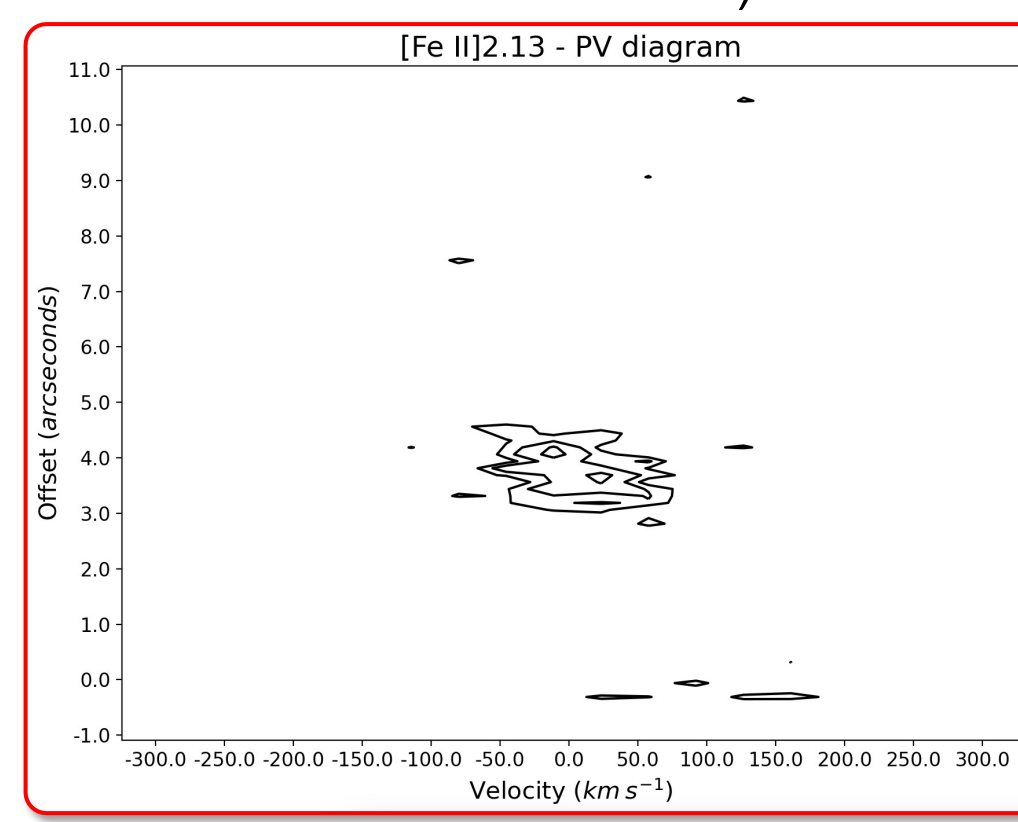
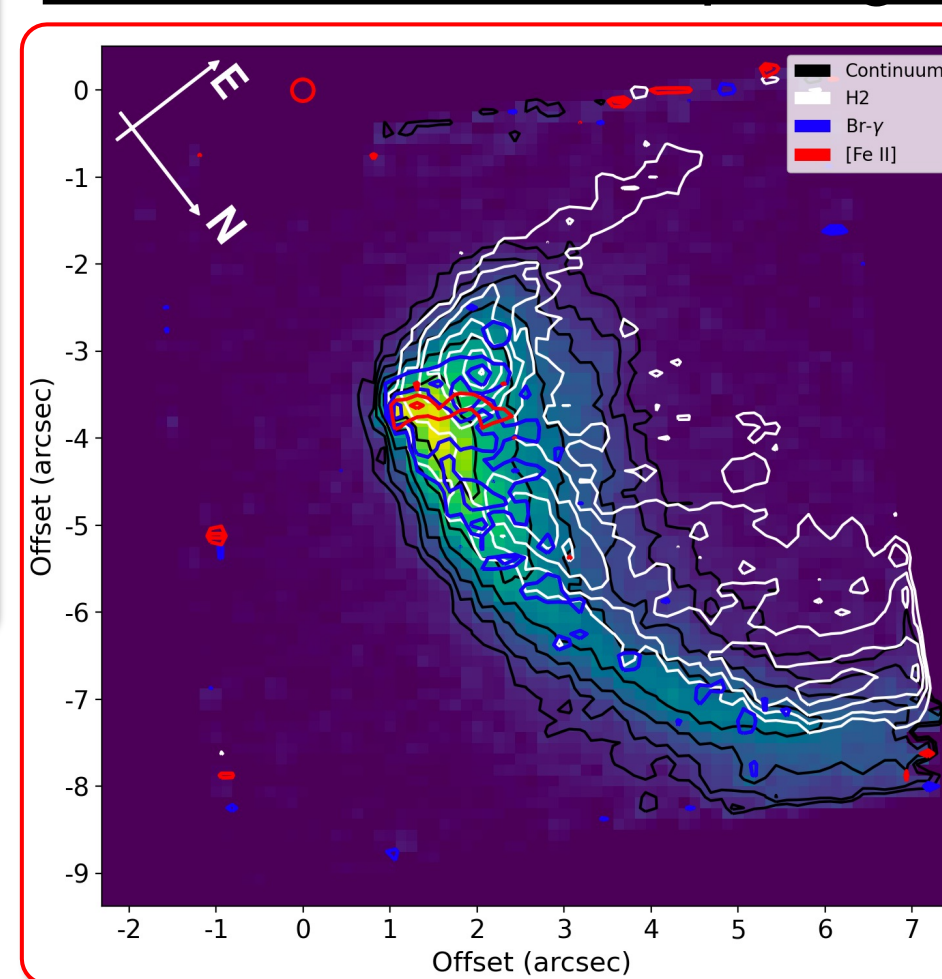


Fig 10: [Fe II] 2.13 PV diagram. Contours start at  $3\sigma$  and increase by factors of 1.5 ( $\sigma = 36.20 \times 10^{-23} \text{ W cm}^{-2} \mu\text{m}^{-1} \text{ pixel}^{-1}$ )

### Jet tracers and sample figure from MUSE data:



- [Fe II]** traces the fast-moving jet, **Br- $\gamma$**  traces accretion processes and **H2** traces the jet cavity and slower moving parts of the jet.

Fig 11: [Fe II] 2.13 (red), Br- $\gamma$  (blue) and H2 2.12 (white) emission overlaid on continuum (black). Emission from different atoms and molecules trace different aspects of the jet.

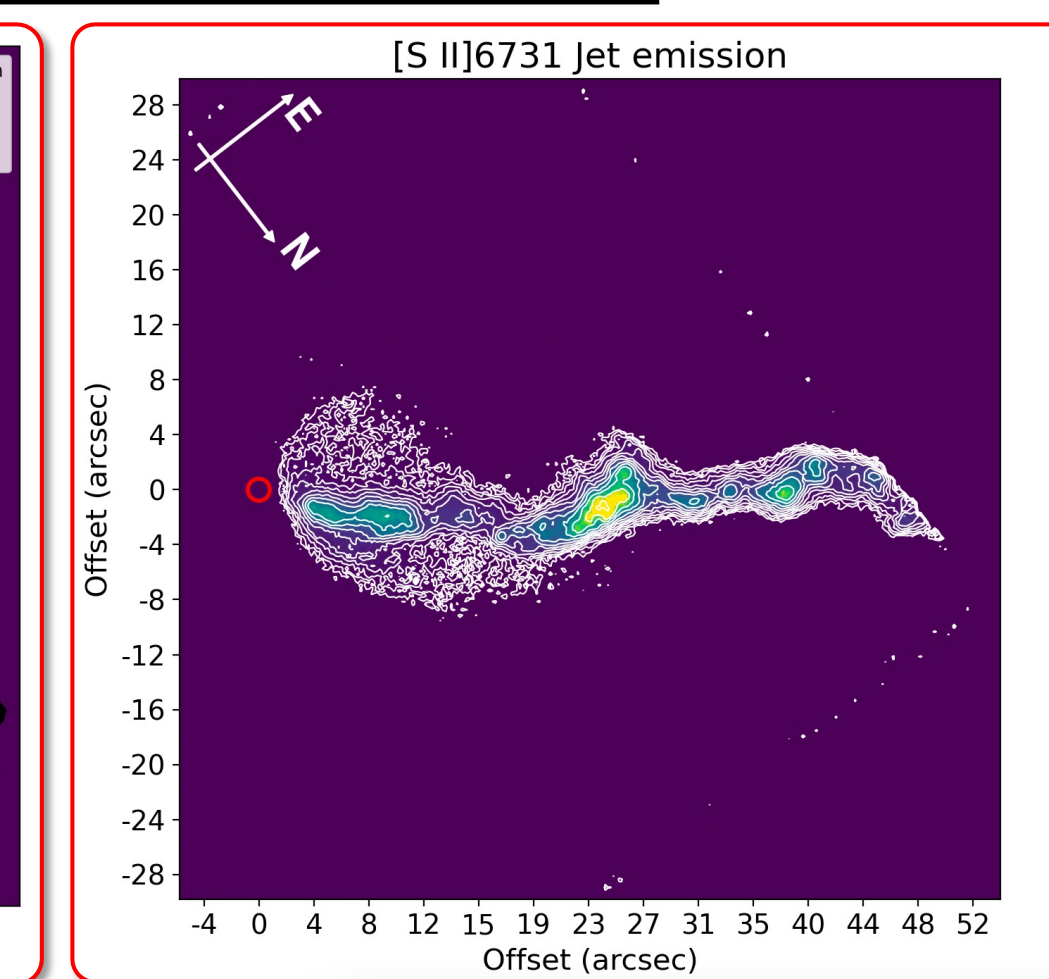


Fig 12: [S II] 6731  $\text{\AA}$  emission contour plot. Red circle marks ALMA mm continuum peak. Contours start at  $5\sigma$  and increase in factors of 1.5 ( $\sigma = 5.22 \times 10^{-27} \text{ W cm}^{-2} \text{\AA}^{-1} \text{ pixel}^{-1}$ )

## Conclusions & Future Work

- Complete the **kinematical and morphological study** of jet - Measurements of the collimation, rotation and structure (kinematical and physical) of the jet will provide constraints on theoretical jet launching models; The Disk-wind model proposes that the jet is launched from a wide range of disk radii while the X-wind model proposes the jet is launched from a singular radius on the disk, known as the X-point.
- Complete a **diagnostic study** of the jet, identifying if the jet shows stratification in density, temperature and ionisation fraction, and a jet efficiency study.
- Complete a **proper motion study** of the jet with Dr Fernando Comerón at ESO-Garching.
- Investigate the jet-disk interaction and subsequently the impact of jet launching on the planet forming regions of the disk.